Research article

Power spectral density and similarity analysis of COVID-19 mortality waves across countries

Elias Manjarrez [a,*], Erick F. Delfin [a], Saul M. Dominguez-Nicolas [b,c], Amira Flores [a]

[a] *Instituto de Fisiología, Benemérita Universidad Autónoma de Puebla, 14 Sur 6301, Colonia San Manuel, Apartado Postal 406, CP 72570, Puebla, Puebla, Mexico*
[b] *Centro de Investigación de Micro y Nanotecnología, Universidad Veracruzana, Calzada Ruiz Cortines 455, Boca del Rio, Veracruz, 94294, Mexico*
[c] *Facultad de Ingeniería Eléctrica y Electrónica, Universidad Veracruzana, Calzada Ruiz Cortines 455, Boca del Rio, Veracruz, 94294, Mexico*

A B S T R A C T

Background: During the COVID-19 pandemic, the Johns Hopkins University Center for Systems Science and Engineering (CSSE) established a comprehensive database detailing daily mortality rates across countries. This dataset revealed fluctuating global mortality trends attributable to COVID-19; however, the specific differences and similarities in mortality patterns between countries remain insufficiently explored. Consequently, this study employs Fourier and similarity analyses to examine these patterns within the frequency domain, thereby offering novel insights into the dynamics of COVID-19 mortality waves across different nations.
Methods: We employed the Fast Fourier transform to calculate the power spectral density (PSD) of COVID-19 mortality waves in 199 countries from January 22, 2020, to March 9, 2023. Moreover, we performed a cosine similarity analysis of these PSD patterns among all the countries.
Results: We identified two dominant peaks in the grand averaged PSD: one at a frequency of 1.15 waves per year (i.e., one wave every 10.4 months) and another at 2.7 waves per year (i.e., one wave every 4.4 months). We also found a cosine similarity index distribution with a skewness of -0.54 and a global median of cosine similarity index of 0.84, thus revealing a remarkable similarity in the dominant peaks of the COVID-19 mortality waves.
Conclusion: These findings could be helpful for planetary health if a future pandemic of a similar scale occurs so that effective confinement measures or other actions could be planned during these two identified periods.

1. Introduction

Although the Spanish flu occurred over 100 years ago [1–3], no nation was prepared for a pandemic of this scale in modern times. This lack of preparation and the variety of transportation systems between nations contributed to the COVID-19 pandemic spreading rapidly and affecting all countries worldwide. This, in turn, caused a total collapse in healthcare systems in many countries from the onset of the disease [4]. Another contributing factor was the high virulence of the SARS-CoV-2 virus, which, combined with the massive global population, facilitated a dramatic increase in infections in many countries within weeks [5]. Hence, the COVID-19 pandemic resulted in over 7 million deaths worldwide. In this context, the number of fatalities proves that the pandemic control was unsuccessful without vaccination. Therefore, a systematic analysis of COVID-19 mortality patterns worldwide would be helpful for future generations if a new pandemic of a similar scale could occur.

* Corresponding author. Instituto de Fisiología, Benemérita Universidad Autónoma de Puebla, 14 sur 6301, Col. San Manuel A.P. 406, C.P. 72570, Puebla, Pue, Mexico.,
E-mail addresses: elias.manjarrez@correo.buap.mx, eliasmanjarrez@gmail.com (E. Manjarrez).

2. Background

Fortunately, it is now possible to obtain data on the daily number of SARS-CoV-2 infections, active cases, and COVID-19 deaths worldwide thanks to databases such as "Worldometer" and Johns Hopkins University CSSE [4]. These databases were created to facilitate future studies on the factors contributing to the virus's spread. For this reason, infections and confirmed COVID-19 deaths have been geographically mapped in space and time [4,5]. In addition, data on climatic conditions, population density, population composition, and human travel patterns have also been collected.

2.1. Literature review

Many studies have employed the Johns Hopkins University CSSE database and other databases to investigate various factors influencing the COVID-19 pandemic. These factors include correlations between age and gender on COVID-19 incidence [6] and the interplay between tourism and the virus's spread [7]. Additionally, research has examined the relationship between weather conditions, air pollution, SARS-CoV-2 transmission [8], and the impact of heat waves on the pandemic [9].

Qualitative observation of the graphs generated by the Johns Hopkins University CSSE database revealed that death waves shared similar wave patterns in several countries. However, notable differences existed in various countries. For instance, a previous study examined whether there are similarities in the graphs of COVID-19 mortality rates between Canadian provinces and the American States [10]. Surprisingly, these authors found that most provinces and states are dissimilar in cumulative rates of COVID-19 mortality from January to December 2020 [10], even the close ubication of the studied provinces. This led us to hypothesize that a systematic similarity analysis of worldwide COVID-19 deaths in the frequency domain could help characterize global COVID-19 mortality waves in detail. In this context, our approach is original. Moreover, to our knowledge, we emphasize that no similar reports in the literature in this field examined this novel hypothesis.

Therefore, the objectives of this study were: 1) to use the Johns Hopkins University CSSE database to characterize the power spectral density (PSD) of the worldwide mortality waves caused by COVID-19, and 2) to perform a similarity index analysis of these PSD graphs among countries.

We utilized the PSD methodology because it can quantitatively identify the dominant frequencies of mortality waves more precisely than the qualitative observation of the Johns Hopkins University CSSE COVID-19 database. Additionally, we employed the cosine similarity analysis to precisely compare these dominant frequencies across different countries, thereby elucidating cross-national variations in COVID-19 mortality patterns.

3. Methods

We employed the Johns Hopkins University CSSE COVID-19 database on GitHub.com (full_data.csv) to obtain the COVID-19 daily death counts for n = 229 countries from January 22, 2020, to March 9, 2023.

3.1. Inclusion and exclusion criteria

This is a retrospective observational study in which we analyzed daily COVID-19 death time series from 199 countries to obtain a PSD. We excluded 30 countries due to low COVID-19 deaths and the inability to obtain a peak in the PSD from their time series.

3.2. Power spectral density (PSD) and cosine similarity index analysis

The PSD is obtained from the Fourier transform and its complex conjugate. The PSD describes power distribution across different frequencies (i.e., in the frequency domain). MATLAB was used to calculate the PSD of each country's time series of COVID-19 death counts as follows:

Power Spectral Density for country i = PSD_i where i = 1 to n

Because the PSD graphs have a characteristic shape that could be compared among countries, the PSD data for each country i was then used as a vector defined as:

$PSD_i = (Y1, Y2, \ldots, Yn)_i$,

where Y1, Y2, .., Yn are the PSD values in the vertical axis of a PSD graph. Hence, we computed the cosine similarity index between all pairs of countries i and j worldwide (n = 199 countries) with these PSD vectors. This was the algorithm employed:

Cosine_Similarity_Index (i,j) = dot (PSD_i, PSD_j) / (norm $((PSD_i)^* (PSD_j))$)

These cosine similarity indexes were plotted on a similarity matrix map to identify countries with notable differences in similarity index compared to the majority.

Table 1

The group of 199 countries analyzed in the present study and listed in alphabetical order. Countries highlighted in green (n = 17) correspond to those nations with PSDs of low cosine similarity index below 0.71. The other countries highlighted in yellow (n = 188) correspond to those nations with PSDs of a high cosine similarity index above 0.71.

1) Afghanistan	41) Chile	81) Guinea-Bissau	121) Mauritius	161) Saudi Arabia
2) Albania	**42) China**	82) Guyana	122) Mexico	162) Senegal
3) Algeria	43) Colombia	83) Haiti	123) Moldova	163) Serbia
4) Andorra	**44) Comoros**	84) Honduras	124) Monaco	164) Seychelles
5) Angola	45) Congo	**85) Hong Kong**	125) Mongolia	**165) Sierra Leone**
6) Anguilla	46) Costa Rica	86) Hungary	126) Montenegro	166) Singapore
7) Antigua and Barbuda	47) Cote d'Ivoire	87) Iceland	**127) Montserrat**	167) Slovakia
8) Argentina	48) Croatia	88) India	128) Morocco	168) Slovenia
9) Armenia	49) Curacao	89) Indonesia	129) Mozambique	169) Somalia
10) Aruba	50) Cyprus	90) Iran	130) Myanmar	170) South Africa
11) Australia	51) Czechia	91) Iraq	131) Namibia	171) South Korea
12) Austria	52) Dem. Rep of Congo	92) Ireland	132) Nepal	172) South Sudan
13) Azerbaijan	53) Denmark	93) Isle of Man	133) Netherlands	173) Spain
14) Bahamas	**54) Djibouti**	94) Israel	134) New Caledonia	174) Sri Lanka
15) Bahrain	55) Dominica	95) Italy	135) New Zealand	175) Sudan
16) Bangladesh	56) Dominican Republic	96) Jamaica	136) Nicaragua	176) Sweden
17) Barbados	57) Ecuador	97) Japan	137) Niger	177) Switzerland
18) Belarus	58) Egypt	98) Jordan	138) Nigeria	178) Syria
19) Belgium	59) El Salvador	99) Kazakhstan	139) North Macedonia	179) Taiwan
20) Belize	60) Equatorial Guinea	100) Kenya	140) Norway	180) Tajikistan
21) Benin	61) Eritrea	**101) Kiribati**	141) Oman	**181) Tanzania**
22) Bermuda	62) Estonia	102) Kosovo	142) Pakistan	182) Thailand
23) Bhutan	63) Eswatini	103) Kuwait	**143) Palau**	183) Togo
24) Bolivia	64) Ethiopia	104) Kyrgyzstan	144) Palestine	184) Trini. and Tobago
25) Bonaire S. E. and Saba	**65) Faeroe Islands**	105) Laos	145) Panama	185) Tunisia
26) Bosnia and Herzegovina	66) Fiji	106) Latvia	146) Papua New Guinea	186) Turkey
27) Botswana	67) Finland	107) Lebanon	147) Paraguay	187) Turks and C. Islands
28) Brazil	68) France	108) Lesotho	148) Peru	188) Uganda
29) British Virgin Islands	**69) French Polynesia**	109) Liberia	149) Philippines	189) Ukraine
30) Brunei	70) Gabon	110) Libya	150) Poland	190) U. Arab Emirates
31) Bulgaria	71) Gambia	111) Liechtenstein	151) Portugal	191) United Kingdom
32) Burkina Faso	72) Georgia	112) Lithuania	152) Qatar	192) United States
33) Burundi	73) Germany	113) Luxembourg	153) Romania	193) Uruguay
34) Cambodia	74) Ghana	114) Madagascar	154) Russia	194) Uzbekistan
35) Cameroon	**75) Gibraltar**	115) Malawi	155) Rwanda	195) Venezuela
36) Canada	76) Greece	116) Malaysia	156) Saint Kitts and Nevis	196) Vietnam
37) Cape Verde	**77) Greenland**	117) Maldives	157) Saint Lucia	197) Yemen
38) Cayman Islands	78) Grenada	118) Mali	158) S. Vinc. and the Gre.	198) Zambia
39) Central African Rep.	79) Guatemala	119) Malta	**159) San Marino**	199) Zimbabwe
40) Chad	80) Guinea	120) Mauritania	160) Sao Tome and Princ.	

3.3. Statistical analysis

Finally, we obtained a histogram of these cosine similarity indexes to identify the type of statistical distribution for the data. Then, skewness was calculated with the formula for Pearson's second coefficient [11] as follows:

Skewness = 3 (mean - median)/(standard deviation)

For statistical comparison, we separated two groups of cosine similarity index using a threshold "Th" defined by "Th = mean-std," where "std" is the standard deviation. This threshold helped identify countries with a low cosine similarity index below "mean-std" and countries with a high cosine similarity index above "mean-std." Because data were not normally distributed, we employed a non-parametric Mann-Whitney U test to compare the incidence between these two groups of cosine similarity indexes.

4. Results

We analyzed the daily COVID-19 death toll in 199 countries from January 22, 2020, to March 9, 2023, using data from the Johns Hopkins University CSSE database. Following an alphabetic order, we numbered the countries from 1 to 199, as illustrated in Table 1. We calculated the PSD of these time series per country. Fig. 1A shows examples of time series from eight countries, whereas Fig. 1B shows the respective PSD. Note that some countries exhibit a dominant peak around a frequency of one peak per year. After obtaining the PSD for all the countries listed in Table 1, we calculated the grand average of all PSD (n = 199 countries), shown in Fig. 2. In this global PSD, there are two dominant peaks of COVID-19 mortality waves, the first occurring at a frequency of 1.15 peaks per year and the second at 2.7 peaks per year.

After examining the examples in Fig. 1B, we noted some similarities in the PSD shape among these eight countries, which suggested that there would probably also be differences in the PSD shape among all 199 countries. Therefore, we computed the cosine similarity index between the PSD of all pairs of countries worldwide. The cosine similarity indexes obtained from PSD-shape comparisons are shown in the cosine similarity index matrix in Fig. 3. The consecutive numbers in the horizontal and vertical axes represent the number assigned to each country according to Table 1. For clarity, we obtained the histogram of all cosine similarity indexes illustrated in Fig. 3. Such a histogram is shown in Fig. 4. It demonstrates the distribution of these cosine similarity indexes. The reader can observe that this distribution is negatively skewed. We calculated this distribution's global cosine similarity index parameters, obtaining mean = 0.82, median = 0.84, mode = 0.87, standard deviation = std = 0.11, and skewness = −0.54.

After inspecting the colors in Fig. 3, we can note some lines in the "green" color spectrum. These lines correspond to values below a
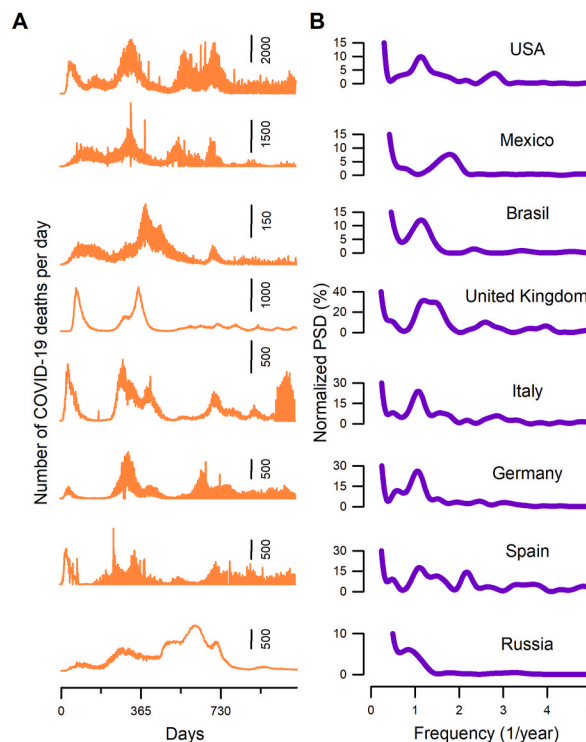

Fig. 1. Examples of COVID-19 mortality waves and their power spectral density (PSD). **A.** Examples of time series showing a high number of COVID-19 deaths per day from eight countries. **B.** Normalized PSD is calculated from the time series shown in the left panel. Note that these countries exhibit a dominant peak around a frequency of one peak per year.
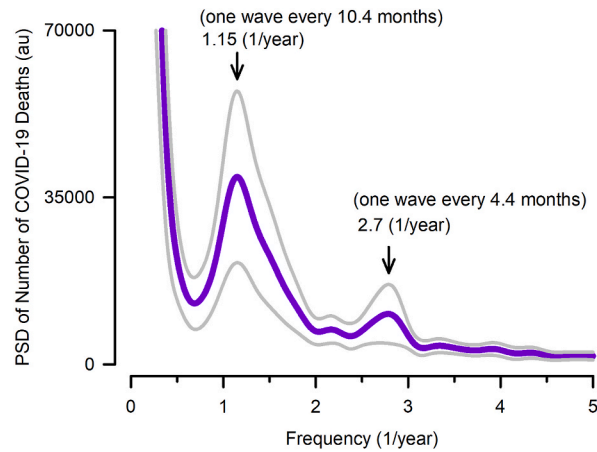
Fig. 2. Global COVID-19 mortality waves worldwide. The purple trace is the grand average of the power spectral density (PSD) obtained from the COVID-19 mortality time series for 199 countries. The traces in grey color represent the standard deviation. Note the two dominant COVID-19 mortality waves occurring at frequencies of 1.15 waves/year (i.e., one wave every 10.4 months) and 2.7 waves/year (i.e., one wave every 4.4 months). (For interpretation of the references to color in this figure legend, the reader is referred to the Web version of this article.)
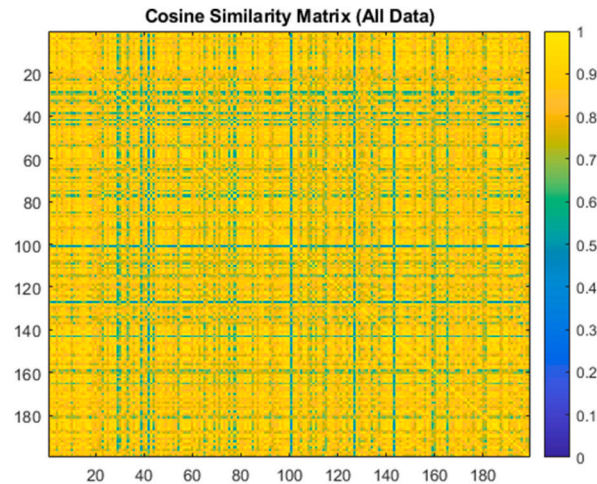

Fig. 3. A cosine similarity matrix for COVID-19 mortality was obtained by comparing all pairs of power spectral density (PSD) graphs for 199 countries listed in Table 1. The right vertical bar represents the cosine similarity index scale from 0 to 1. The numbers on the horizontal and vertical axes of this matrix represent the countries listed in alphabetical order in Table 1. Matrix regions shaded towards yellow indicate pairs of countries with high PSD similarity, while regions shaded towards green indicate low similarity.

cosine similarity index of 0.71, i.e., below the threshold Th = mean-std = 0.82–0.11 = 0.71 of the negatively skewed distribution shown in Fig. 4. We found that these "green" color spectrum lines correspond to 17 countries, as highlighted in green in Table 1. Some examples of the COVID-19 mortality time series and PSD obtained from these countries are illustrated in Fig. 5. A notable qualitative characteristic of these COVID-19 mortality time series in Fig. 5A is that the number of COVID-19 deaths per day does not exhibit COVID-19 mortality waves as those illustrated in Fig. 1A. Another feature of these countries in Fig. 5A is that they exhibited COVID-19 mortality waves in the PSD with multiple peaks (Fig. 5B), thus exhibiting a different behavior in the COVID-19 mortality waves. For instance, China exhibited multiple dominant peaks and fewer COVID-19 deaths (see first panel of Fig. 5B). Fig. 6 is the grand average of the PSD obtained from these 17 countries with a cosine similarity index below 0.71. Note the absence of the two dominant peaks found in the global grand average of the PSD previously shown in Fig. 2.

Moreover, we found n = 182 countries exhibiting a high cosine similarity index above the threshold Th = mean-std = 0.71, which can be identified as those values in the "yellow" color spectrum in Fig. 3. The grand average of the PSD for these 182 countries is shown in Fig. 7.

Finally, we examined whether there is a statistically significant difference in the number of counts related to cosine similarity indexes below Th = 0.71 versus those associated with cosine similarity indexes above Th = 0.71. Both data groups are illustrated with parentheses in Fig. 4. A non-parametric Mann-Whitney *U* test revealed a statistically significant difference $p < 0.0001$ between both
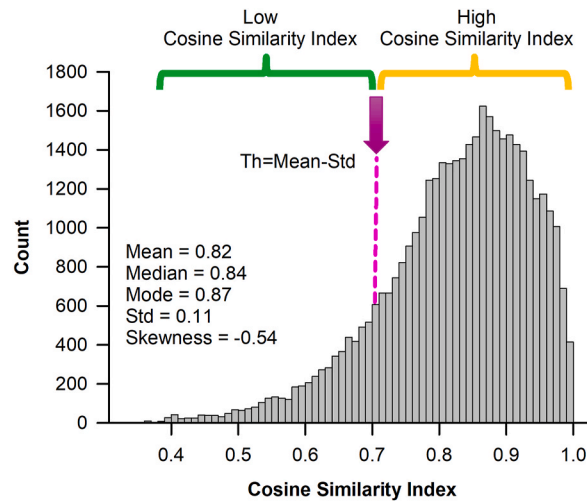
Fig. 4. The histogram of the cosine similarity indexes was obtained from the cosine similarity index matrix shown in Fig. 3. This histogram shows a negatively skewed distribution of the cosine similarity indexes for 199 countries with a skewness of −0.54. The formula Th = Mean-Std was used to calculate the threshold "Th" to separate a data group with low cosine similarity (green parenthesis) and a data group with high cosine similarity (yellow parenthesis). Std is for standard deviation. (For interpretation of the references to color in this figure legend, the reader is referred to the Web version of this article.)
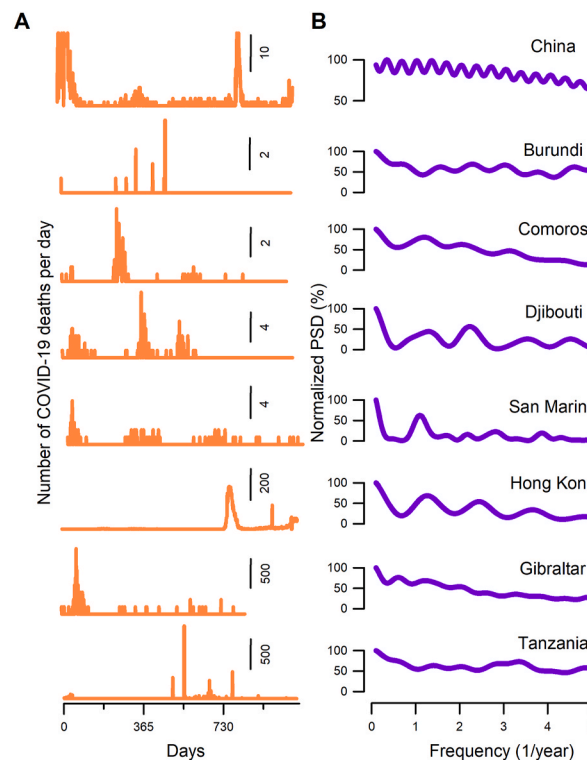

Fig. 5. It has the same format as Fig. 1 but for eight countries with a cosine similarity index below the threshold = mean-std = 0.71. **A.** Examples of time series showing a relatively low number of COVID-19 deaths per day from eight countries. **B.** Normalized power spectral density (PSD) is calculated from the time series shown in the left panel. These countries exhibit a multi-peak behavior in their PSD, occurring at different frequencies.
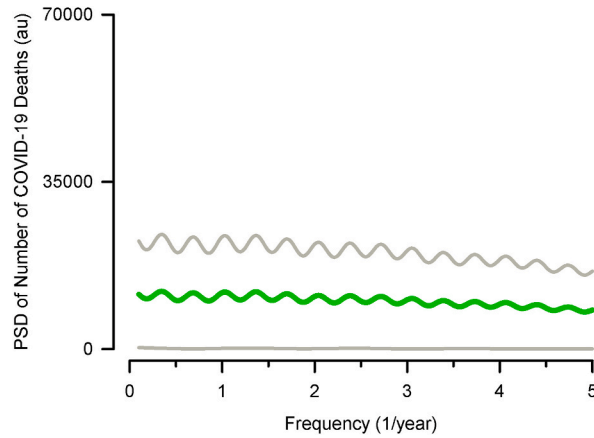
Fig. 6. It has the same format as Fig. 2, but the grand average of the power spectral density (PSD) was obtained from 17 countries that exhibited a similarity index below 0.71. Note a multipeak behavior in the COVID-19 mortality waves occurring at different frequencies from 0.4 to 4.7 COVID-19 mortality waves per year.
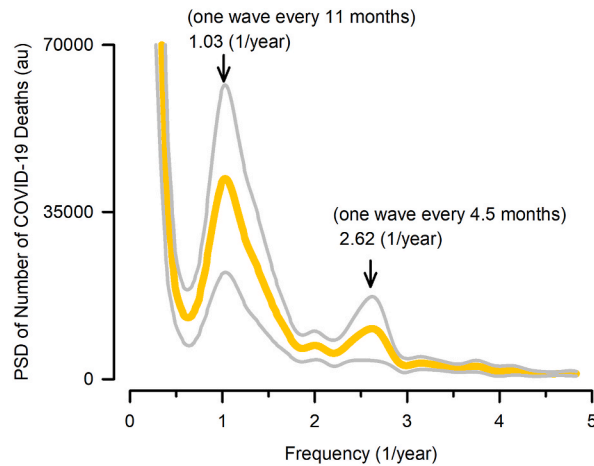

Fig. 7. It has the same format as Fig. 2 but for n = 182 countries with a cosine similarity index above the threshold = mean-std = 0.71. The averaged power spectral density (PSD) for these 182 countries still exhibits two dominant peaks at similar frequencies of 1.03 and 2.62 peaks per year, as the grand averaged PSD for 199 countries.

datasets. This result reveals that it helped define a cosine similarity index threshold of mean-std = 0.71 as a criterion to justify the grand averaged PSD of countries with higher (Fig. 7) and lower (Fig. 6) cosine similarity indexes.

5. Discussion

We analyzed the time series of COVID-19 mortality due to COVID-19 with a PSD. We identified two dominant peaks in the grand average of the PSD of 199 countries: one at a frequency of 1.15 waves per year (i.e., one wave every 10.4 months) and another at 2.7 waves per year (i.e., one wave every 4.4 months). After performing a cosine similarity analysis in the PSD shape for all countries, we found that most of these countries, n = 182, exhibited a similar PSD shape with a high cosine similarity index above the threshold Th = mean-std = 0.71, with two dominant peaks: one at 1.03 (i.e., one wave every 11 months) and another at 2.62 waves per year (i.e., one wave every 4.5 months). However, we found that n = 17 countries exhibited a distinct PSD with a low cosine similarity index below the threshold Th = mean-std = 0.71, with the feature that they exhibited a multipeak PSD shape.

We could speculate that the two COVID-19 mortality waves occurring at a periodicity of 11 months and 4.5 months may correlate to the holiday periods, in which higher inter-country and intra-country human mobility exists. This suggestion aligns with mathematical models predicting the impact of human mobility on epidemics spread during holidays. These models highlight that while inter-regional mobility could trigger epidemic spread, the diffusion effect of intra-regional mobility was primarily responsible for outbreaks within a city [12]. In this context, it is possible that the differences in the COVID-19 mortality PSD waves among countries could be due to differences in governmental regulations, population density, weather conditions, and shared population activities without

confinement.

The observed similarities in the COVID-19 mortality PSD patterns among most countries validate the global nature of the pandemic, reflecting potential common factors influencing COVID-19 mortality rates (Figs. 1 and 3). However, the notable differences in PSD patterns among a subset of countries (Fig. 6) versus another set of countries (Fig. 7) highlight the potential influence of different local factors, such as public health policies. Other factors, such as healthcare system resilience and population behavior, among other unknown factors, could also influence the differences in the COVID-19 mortality waves. Future studies will be necessary to uncover these factors. In this context, future research should identify other pandemic variables exhibiting a periodicity every 11 and 4.5 months.

We searched the literature for biological variables related to this periodicity every 11 and 4.5 months. We only found that infections in aquatic parasitic copepods (***Ch. Quaternia***) are increased with a periodicity of every 11 and 3 months in the oceanographic conditions of the Pacific Ocean associated with the 2015–2016 El Niño [13]. The readers may note the parallelism in the periodicity of infection parameters in ***Ch. Quaternia*** and the periodicity of COVID-19 mortality due to SARS-CoV-2 infection in humans.

The findings from both the literature [4–9] and the current study underscore the importance of global data collection and analysis tools, such as the Johns Hopkins University CSSE database, in monitoring and understanding pandemic trends. The variability in COVID-19 mortality patterns across countries emphasizes the need for tailored public health responses considering local conditions and capabilities. Furthermore, identifying common COVID-19 mortality waves suggests potential areas for international collaboration in pandemic preparedness and response in case a similar pandemic of a similar scale could occur. In this context, our study offers a quantitative characterization of mortality waves during the COVID-19 pandemic, which could be helpful for future modeling studies and provide critical lessons for managing future global health crises.

5.1. Limitations

A limitation of our study is the possibility that the counts of daily COVID-19 deaths are over- and under-estimated. Reports suggest that COVID-19 deaths were not counted adequately during the pandemic in several countries [14]. Another limitation is that we did not analyze correlations with potential factors that could influence the high and low cosine similarity in the periodicity of the COVID-19 mortality waves, such as governmental regulations, population density, weather conditions, and shared population activities without confinement, among other factors.

5.2. Future work

In addition, future modeling strategies will be necessary to understand the dynamic of the pandemic in different contexts and comorbidities, such as the fractal fractional COVID-19 models [15] or novel stochastic SIRS (susceptible, infectious, recovered) epidemic models [16,17]. Furthermore, other regional studies in different countries, such as South Africa [18–20], Portugal [21], Turkey [22], and Italy [23], could be analyzed in the context of the PSD or cosine similarity index methods.

6. Conclusion

We conclude that the PSD analysis of COVID-19 mortality time series across 199 countries revealed patterns in COVID-19 mortality waves characterized by two dominant peaks at frequencies of 1.15 and 2.7 waves per year. Moreover, the quantitative analysis using the cosine similarity index to compare the PSD shapes among countries uncovers a broad similarity in COVID-19 mortality patterns, with a significant portion of countries exhibiting high cosine similarity indices. However, it also identifies a subset of countries with distinct COVID-19 mortality wave patterns, as indicated by lower cosine similarity indices and multiple peaks in their PSDs. This divergence suggests variability in how different populations were impacted by and responded to the pandemic. Furthermore, the methodology employed here, using PSD analysis and the cosine similarity index, offers a novel approach to quantitatively assess global and local patterns of COVID-19 mortality, complementing previous qualitative observations found in the Johns Hopkins University CSSE database [4]. Hence, our findings could contribute to planetary health by guiding effective confinement measures and other actions during future pandemics of similar scale, particularly in the two identified periods.

Funding statement

Data availability statement

We obtained data for this study from the publicly available repository of the Johns Hopkins University CSSE database. Readers can access the data file (full_data.csv) at the following link:
https://github.com/owid/covid-19-data/tree/master/public/data/jhu.

CRediT authorship contribution statement

Elias Manjarrez: Writing – review & editing, Writing – original draft, Visualization, Validation, Supervision, Software, Resources, Project administration, Methodology, Investigation, Funding acquisition, Formal analysis, Data curation, Conceptualization. **Erick F. Delfin:** Investigation, Formal analysis. **Saul M. Dominguez-Nicolas:** Investigation, Formal analysis. **Amira Flores:** Investigation, Formal analysis, Validation.

Declaration of competing interest

The authors declare the following financial interests/personal relationships which may be considered as potential competing interests: Elias Manjarrez reports article publishing charges was provided by Benemérita Universidad Autónoma de Puebla. If there are other authors, they declare that they have no known competing financial interests or personal relationships that could have appeared to influence the work reported in this paper.

References

[1] P. Berche, The Spanish flu, Presse Med. 51 (3) (2022) 104127, https://doi.org/10.1016/j.lpm.2022.104127.

[2] F. Lista, M.S. Peragallo, R. Biselli, R. De Santis, S. Mariotti, R. Nisini, R. D'Amelio, Have diagnostics, therapies, and vaccines made the difference in the pandemic evolution of COVID-19 in comparison with "Spanish flu", Pathogens 12 (7) (2023) 868, https://doi.org/10.3390/pathogens12070868.

[3] Á. Doran, C.L. Colvin, E. McLaughlin, What can we learn from historical pandemics? A systematic review of the literature, Soc. Sci. Med. 342 (2024) 116534, https://doi.org/10.1016/j.socscimed.2023.116534, 1982.

[4] E. Dong, J. Ratcliff, T.D. Goyea, A. Katz, R. Lau, T.K. Ng, B. Garcia, E. Bolt, S. Prata, D. Zhang, R.C. Murray, M.R. Blake, H. Du, F. Ganjkhanloo, F. Ahmadi, J. Williams, S. Choudhury, L.M. Gardner, The Johns Hopkins university center for systems science and engineering COVID-19 dashboard: data collection process, challenges faced, and lessons learned, Lancet Infect. Dis. 22 (12) (2022 Dec) e370–e376, https://doi.org/10.1016/S1473-3099(22)00434-0. Epub 2022 Aug 31. Erratum in: Lancet Infect Dis. 2022 Nov;22(11):e310. PMID: 36057267; PMCID: PMC9432867.

[5] F.S. Hass, J.J. Arsanjani, The geography of the Covid-19 pandemic: a data-driven approach to exploring geographical driving forces. https://doi.org/10.3390/ijerph18062803, 2021.

[6] D. Hu, X. Lou, N. Meng, Z. Li, Y. Teng, Y. Zou, F. Wang, Influence of age and gender on the epidemic of COVID-19 : evidence from 177 countries and territories-an exploratory, ecological study, Wien Klin. Wochenschr. 133 (7–8) (2021 Apr) 321–330, https://doi.org/10.1007/s00508-021-01816-z. Epub 2021 Feb 5. PMID: 33547492; PMCID: PMC7864622.

[7] D. Hu, N. Meng, X. Lou, Z. Li, Y. Teng, Y. Zou, F. Wang, Significantly correlation between tourism and COVID-19: evidence from 178 countries and territories, Journal of infection in developing countries 16 (2) (2022) 283–290, https://doi.org/10.3855/jidc.14929.

[8] R. Xu, H. Rahmandad, M. Gupta, C. DiGennaro, N. Ghaffarzadegan, H. Amini, M.S. Jalali, Weather, air pollution, and SARS-CoV-2 transmission: a global analysis, Lancet Planet. Health 5 (10) (2021) e671–e680, https://doi.org/10.1016/S2542-5196(21)00202-3.

[9] X. Lian, J. Huang, H. Li, Y. He, Z. Ouyang, S. Fu, Y. Zhao, D. Wang, R. Wang, X. Guan, Heat waves accelerate the spread of infectious diseases, Environ. Res. 231 (Pt 2) (2023) 116090, https://doi.org/10.1016/j.envres.2023.116090.

[10] T.W. Myroniuk, M. Teti, E. Schatz, I. David, Similarities in COVID-19 mortality between Canadian provinces and American states before vaccines were available, Can. Stud. Popul. 50 (1) (2023) 2, https://doi.org/10.1007/s42650-023-00073-x.

[11] G.U. Yule, M.G. Kendall, An Introduction to the Theory of Statistics, fourteenth ed., Griffin, 1911 rev.).

[12] H. Li, J. Huang, X. Lian, Y. Zhao, W. Yan, L. Zhang, L. Li, Impact of human mobility on the epidemic spread during holidays, Infectious Disease Modelling 8 (4) (2023) 1108–1116, https://doi.org/10.1016/j.idm.2023.10.001.

[13] A.M. Santana-Piñeros, Y. Cruz-Quintana, A.L. May-Tec, G. Mera-Loor, M.L. Aguirre-Macedo, E. Suárez-Morales, D. González-Solís, The 2015-2016 El Niño increased infection parameters of copepods on Eastern Tropical Pacific dolphinfish populations, PLoS One 15 (5) (2020) e0232737. https://doi:10.1371/journal.pone.0232737.

[14] J.P.A. Ioannidis, Over- and under-estimation of COVID-19 deaths, Eur. J. Epidemiol. 36 (6) (2021) 581–588, https://doi.org/10.1007/s10654-021-00787-9.

[15] H. Khan, J. Alzabut, O. Tunç, M.K.A. Kaabar, A fractal–fractional COVID-19 model with a negative impact of quarantine on the diabetic patients, Results in Control and Optimization 10 (2023) 100199, https://doi.org/10.1016/j.rico.2023.100199.

[16] A. Alkhazzan, J. Wang, Y. Nie, H. Khan, J. Alzabut, A novel SIRS epidemic model for two diseases incorporating treatment functions, media coverage, and three types of noise, Chaos, Solit. Fractals 181 (2024) 114631, https://doi.org/10.1016/j.chaos.2024.114631.

[17] S. Hussain, E.N. Madi, H. Khan, S. Etemad, S. Rezapour, T. Sitthiwirattham, N. Patanarapeelert, Investigation of the stochastic modeling of COVID-19 with environmental noise from the analytical and numerical point of view, Mathematics 9 (2021) 3122, https://doi.org/10.3390/math9233122.

[18] O. Hirachund, C. Pennefather, M. Naidoo, Mortality trends during the first three waves of the COVID-19 pandemic at an urban district hospital in South Africa: a retrospective comparative analysis, S. Afr. Med. J. 114 (2) (2024) e1054, https://doi.org/10.7196/SAMJ.2024.v114i2.1054.

[19] O. Hirachund, C. Pennefather, M. Naidoo, A single-centred retrospective observational analysis on mortality trends during the COVID-19 pandemic, S. Afr. Fam. Pract. 65 (1) (2024) e1–e9, https://doi.org/10.4102/safp.v65i1.5700.

[20] J. Smith-Sreen, B. Miller, A.N. Kabaghe, E. Kim, N. Wadonda-Kabondo, A. Frawley, S. Labuda, E. Manuel, H. Frietas, A.C. Mwale, T. Segolodi, P. Harvey, O. Seitio-Kgokgwe, A.E. Vergara, E.S. Gudo, E.J. Dziuban, N. Shoopala, J.Z. Hines, S. Agolory, M. Kapina, N. Sinyange, M. Melchior, K. Mirkovic, A. Mahomva, S. Modhi, S. Salyer, A.S. Azman, C. McLean, L.P. Riek, F. Asiimwe, M. Adler, S. Mazibuko, V. Okello, A.F. Auld, Comparison of COVID-19 pandemic waves in 10 countries in southern Africa, 2020-2021, Emerg. Infect. Dis. 28 (13) (2022) S93–S104, https://doi.org/10.3201/eid2813.220228.

[21] P.J. Nogueira, Nobre M. de Araújo, C. Elias, R. Feteira-Santos, A.C. Martinho, C. Camarinha, L. Bacelar-Nicolau, A.S. Costa, C. Furtado, L. Morais, J. Rachadell, M.P. Pinto, F. Pinto, A. Vaz Carneiro, Multimorbidity profile of COVID-19 deaths in Portugal during 2020, J. Clin. Med. 11 (7) (2022) 1898, https://doi.org/10.3390/jcm11071898.

[22] A. Ucar, S. Arslan, Estimation of excess deaths associated with the COVID-19 pandemic in istanbul, Turkey, Front. Public Health (2022), https://doi.org/10.3389/fpubh.2022.888123. Jul 25;10:888123.

[23] D. Del Re, L. Palla, P. Meridiani, L. Soffi, M.T. Loiudice, M. Antinozzi, M.S. Cattaruzza, The spread in time and space of COVID-19 pandemic waves: the Italian experience from mortality data analyses, Front. Public Health 12 (2024) 1324033, https://doi.org/10.3389/fpubh.2024.1324033.